Endo-Thal

The official journal of the International Network on Endocrine Complications in Thalassaemia (I-CET)

MRI Assessment of iron overload in thalassemia: an overview

Kavita Saggar[1], Praveen Sobti[2]

[1] Department of Radiodiagnosis and [2] Department of Paediatrics Dayanand Medical College, Ludhiana (India).

MRI Assessment of iron overload in thalassemia: an overview

β thalassemia major is a hereditary hemolytic disorder treated with multiple blood transfusions. The main complication of this treatment is iron overload initially in the reticuloendothelial system, joints and then in all parenchyma, especially the heart, liver, and endocrine glands. Increased iron deposition has a cytotoxic effect, leading to cell death and organ dysfunction. Measures of plasma ferritin levels and hepatic iron level are used for assessing body iron overload. Direct assessment of iron deposition in different organs necessitates tissue biopsy, which is not always possible. Magnetic Resonance Imaging (MRI) is a reliable & non-invasive tool for assessing tissue siderosis. With the advent of increasing options for iron chelation therapy, MRI can guide clinicians to more appropriately tailor chelation therapy to individual patient needs, producing greater efficacy with less toxicity. Future research in MRI monitoring aims at improved prevention of endocrine toxicities, particularly hypogonadotropic hypogonadism and diabetes.

Key words: Magnetic resonance, thalassemia, iron overload, liver, heart, endocrine glands.

Introduction

β-Thalassaemia major is a hereditary haemolytic anaemia that is treated with multiple blood transfusions. A major complication of this treatment is iron overload, which has cytotoxic effect & leads to cell death and organ dysfunction. Chelation therapy, used for iron elimination, requires effective monitoring of the body burden of iron (1).
Many centers rely exclusively on serum ferritin to track somatic iron stores. Whereas trends in serum ferritin remain an important monitoring tool, serum ferritin is a poor marker of iron balance because it varies with inflammation, ascorbate status, and intensity of transfusion therapy. Liver iron measurement by biopsy is more accurate but its invasiveness limits routine screening at most institutions. The desire to replace liver biopsy with a noninvasive test drove the earliest studies on magnetic resonance imaging (MRI) iron quantification (2).

Physics of MRI tissue iron assessment

The use of MRI to estimate tissue iron was conceived in the early 1980s, but did not become practical until MRI technology matured 20 years later (2). The general concept is simple (3). MRI machines can generate images at various observation or "echo" times to vary the contrast among different organs. All organs darken with increasing echo time, but those containing iron darken more rapidly. This is due to the fact that, the magnetic field in a clinical scanner is extremely homogenous, but iron within the tissues creates local magnetic field disturbances that cause the images to darken faster.
T2* represents the echo time necessary for a tissue to become twice as dark. Alternatively, image darkening can be expressed by R2*, its rate of darkening. Some investigators prefer to report R2* values rather than T2* values, because R2* is directly proportional to iron concentration (4, 5). R2* values are simply 1000/T2* and vice versa, making it easily to convert one representation to another (6).
MRI scanners can also collect images suitable for T2 (and R2) analysis instead of T2* analysis, using radiofrequency pulse rather than magnetic gradients to generate images at different echo times. Image analysis and iron quantification is similar whether using R2 or R2* images. R2 images take longer to collect and are used more frequently to evaluate liver iron concentration (LIC) (6). Whereas cardiac T2 imaging is also possible, it is more challenging because of respiratory motion, limiting its widespread acceptance (7).

MRI Field strength

Although most 1.5 Tesla magnets are intrinsically able to perform iron estimation measurements, specialized software and local expertise/training are required for accurate assessment. As a result, some centers have chosen to purchase commercial software or outsource their image analysis to fee-for-service vendors rather than commit the resources to obtain the measurements themselves. Published iron calibration curves are available for liver R2, liver R2*, and cardiac R2* measurements at 1.5 Tesla. Calibration refers to the mathematical association between MRI measurements and underlying tissue iron concentration (7).
Relaxation rates R2 and R2* increase with field strength. Because of the dependency of relaxation rates on field strength, calibration curves obtained at one field strength (e.g., 1.5T) cannot be transferred directly to another field strength (e.g., 3T).
Thus, calibration curves at different field strengths should be derived and validated. Also, whereas 3T imaging provides higher signal to noise than 1.5T, it has theoretical disadvantages for LIC estimation. For example, susceptibility artifacts are worse than at 1.5T, which may degrade GRE image quality. More importantly, owing to faster signal decay at 3T, the maximum quantification limit may be lower than at 1.5T, potentially lowering the utility of 3T scanners for iron quantification (8).

MR methodologies

MR methods for assessing tissue iron can be separated into two groups: signal intensity ratio (SIR) methods and relaxometry methods. Various techniques have been described, including: (a) methods measuring SIR based on T2-weighted (spin-echo) or T2*-weighted (gradient-echo) sequences (9, 10-19), (b) relaxometry methods measuring absolute T2, (c) relaxometry methods measuring absolute T2*, and (d) hybrid relaxometry methods (14, 15, 20-26).

SIR methods

These have been used for the study not only of the liver but also of other organs such as the spleen, pancreas, pituitary gland, bone marrow and abdominal lymph nodes (9, 10, 12, 14,-19, 27). For SIR assessment the signal intensity of the target organ is divided by the signal intensity of a reference tissue (e.g. fat, muscle) or noise. Signal intensity measurements are performed in the same slice by using the region-of-interest (ROI) method. For large organs such the liver, spleen and pancreas more than one ROI is used, positioned in areas lacking vascular structures and movement artefacts (9, 10, 12, 14, 15, 18, 19, 27). The mean signal intensity from the different ROIs is then divided by the signal intensity of the reference tissue (1).
A disadvantage of the SIR methods is that in most cases they use only one echo time (TE) and thus lose their detection sensitivity in tissues with heavy siderosis, where transverse relaxation is much faster than the TE. This occurs particularly in the liver at the upper range of LIC values where signal intensities are widely dispersed (28). *Gandon, et al.* (9) by using an algorithm that combined signal intensity ratios from multiple sequences with different TEs, achieved extension of the detection range up to about 21 mg Fe per gram dry liver tissue, with sensitivity and specificity similar to those of biochemical analysis.

T2 relaxometry methods

These assess T2 relaxation time or R2 (1/T2) by using the Carr-Purcell-Meiboom-Gill (CPMG) spin-echo sequence, which employs multiple (2-32) equidistant refocusing 180° pulses, each followed by an echo (29, 30). Most scanners, by using a pixel-by-pixel, log-linear fitting model, automatically derive the corresponding T2 maps. Signal intensity measurements in the T2 maps correspond to the mean T2 relaxation time of the included voxels (31).
A T2 relaxometry method that received FDA approval for clinical liver iron estimation has recently been developed by *St. Pierre, et al.* This method uses multiple T2-weighted single spin-echo sequences with different TEs acquired in half-Fourier mode to reduce acquisition time. The calculated mean R2 values combined with LIC values, obtained from liver biopsies, are used to create calibration curves (1).

T2* relaxometry methods

These evaluate T2* or R2* by using multiple gradient-echo sequences with different TEs. These methods have been developed to further accelerate acquisition, in order to increase sensitivity and eliminate artefacts related to respiration or cardiac motion. To obtain R2* (1/T2*) values, the signal decay curve is usually fitted with an exponential model: $S=S0e^{-TE/T2*}$, where S is the net image signal intensity, TE is the echo time and S0 is a constant (32). T2* relaxometry methods have been used mainly for myocardial iron assessment and cardiac gating is always applied (23, 32-36). Breath-hold sequences have greatly eliminated motion artefacts (23, 32, 33).

Hybrid relaxometry methods

Hybrid approaches have been applied in high fields and measure both R2 and R2* to calculate the inhomogeneity factor $R2'=R2*-R2$. These approaches assume that R2′ is more specific to mechanisms of relaxation related to iron than R2 (32, 37, 38).

Comparison of the MRI methodologies. SIR versus relaxometry

SIR methods require shorter acquisition times but lack a wide range of iron assessment (26). Relaxometry methods, mainly the T2* method, by using multiple echoes create in and out of phase effects between water and fat transverse magnetization (23). Relaxometry methods, although taking longer, are preferable because they achieve a better sampling of the time domain in which relaxation mechanisms take place and lead to more precise results (26).
MRI studies of individual iron overloaded organs
The degree of siderosis, the crystalline structure of ferritin, the rate of iron elimination under chelation therapy and the degree of ferrioxamine formation are all organ-specific (1). All these parameters may be responsible for differences in the T2 relaxation enhancement induced in the various organs. Individual organs should be considered separately, and the effect of age on iron overload should be taken into account. Higher

survival probabilities have been reported in patients with thalassaemia born in the last 30 years. Patient compliance with treatment regimens and effective chelation therapy are thought to be the main factors associated with improved survival (39). The combination of DFO, deferiprone and the new oral chelators is considered very promising, but will require effective monitoring by non-invasive methods (40). An increasing number of studies have evaluated iron in the various affected organs by MRI (1).

MRI assessment of Liver

For the MRI evaluation of liver siderosis both SIR and relaxometry techniques have been used (10, 21, 32, 41-44). R2 of the liver demonstrates a significant positive correlation with serum ferritin and LIC determined from liver biopsy material (10, 21, 28, 32, 41, 43, 45). Comparative evaluation of hepatic R2 and R2* in iron overloaded patients demonstrates that both parameters correlate closely with LIC (44).
Liver R2* images are the easiest and quickest to collect, but require specialized software to generate R2* and iron estimates. The upper limit of liver iron that can be reliably estimated by R2* depends on scanner specifications, but is generally 30-40 mg/g dry weight at 1.5 Tesla (7).
The relationship of SIR with LIC and serum ferritin varies among studies (14, 15, 41). In most studies R2 and SIR show a better correlation with LIC than with serum ferritin (10, 21, 32, 41-44). This can be explained in part because the HCV-positive thalassaemia patients in the studies had higher serum ferritin levels than those who were HCV-negative (46, 47). Liver R2 shows no association with the hepatic inflammation histological activity index or the type of hepatitis (chronic persistent or chronic active), but is affected by hepatic fibrosis (28, 41, 46).
In iron overload states, over 70% of body iron is found in the liver and LIC has been considered to be the best marker of total body iron burden. Based on the good correlation between hepatic R2 or SIR and LIC a number of recent studies have tested the relationship between siderosis of the liver and other organs. No correlation has been found between liver and pituitary siderosis. 1 With regard to the heart, a correlation with liver siderosis has been found only in cases of heavy myocardial iron deposition (28, 45). This lack of correlation can probably be explained by differences in transferrin receptor concentration, iron kinetics, the crystalline structure of ferritin and the degree of organ inflammation or fibrosis (1). Furthermore, under chelation therapy with DFO intracellular paramagnetic ferrioxamine is formed, which exits slowly from cells unless there is an active excretion pathway as is present in the hepatocytes (48).
Young patients with thalassaemia studied longitudinally have shown absence of substantial improvement in the MR parameters of liver siderosis under different chelation therapy regimens (49). This may be explained by the fact that liver siderosis progresses very fast in thalassaemia patients, and iron overload develops after only 2 years of transfusion therapy (50). Therapy with the most widely used chelating agent is started at the age of about 3 years, and until growth is completed DFO should not exceed a dose of 40 mg/kg per day (51). An early start to monitoring the progress of tissue iron deposition with MRI might be useful in deciding whether to begin

Table 1.

Grading of hepatic iron loading (GE software).

Grades	T2* Value (ms)
Normal	> 6.3
Mild	6.3-2.7
Moderate	2.7-1.4
Severe	<1.4

Figure 1.

Hepatic T2 Map. T2* value of 5.92 ms indicates mild hepatic iron load.*

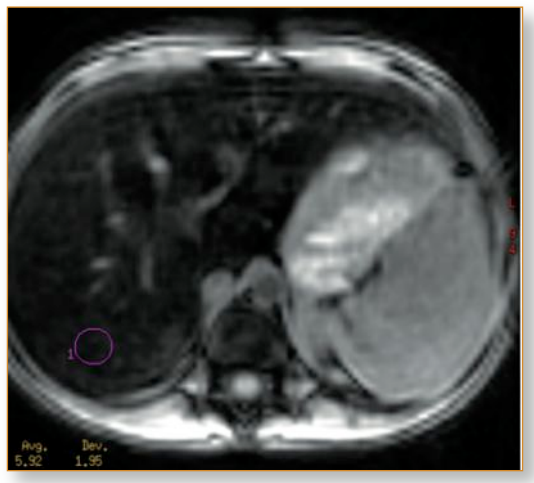

chelation therapy at a younger age and when to introduce new chelating agents (1) (Table 1).
Both T2 and T2* values should be converted to liver biopsy equivalents using established calibration curves. Prospective cardiac risk increases with severe hepatic siderosis. High liver iron (15-20 mg/g dry weight) damages liver parenchyma and increases circulating NTBI levels dramatically. Therefore, the penalty for chelator noncompliance increases at high LICs. LIC values below 5 mg/g can facilitate cardiac iron clearance with deferoxamine and deferasirox; however, no liver iron can be considered "safe" from a cardiac and endocrine perspective and extrahepatic monitoring by MRI is essential (7) (Figure 1).

MRI assessment of cardiac iron

Cardiac R2* (or T2*) is generally measured using the same scanner and software tools as those used for the measurement of liver R2*. It is a little more labor intensive to acquire, but any center with expertise with cardiac scanning should be comfortable planning and executing the examination. Estimates of left ventricular dimensions and function can be obtained at the same time. Cardiac T2* can be converted to cardiac iron concentrations using the following equation (5):

$$Fe = 45(T2^*)-1.22$$

Where Fe is the cardiac iron concentration in milligrams per gram dry weight and T2* is in milliseconds.
Cardiac T2* > 20 milliseconds is considered the lower limit of normal, corresponding to a myocardial iron concentration of 1.16 mg/g. Cardiac T2* values between 10 and 20 milliseconds represent mild to moderate cardiac iron deposition. Patients with a cardiac T2* in this range rarely have heart failure, but chelation should be adjusted to facilitate cardiac iron clearance. Cardiac T2* below 10 milliseconds represents severe cardiac iron loading, with the risk of heart failure increasing sharply as T2* declines. 52 Without intensification of therapy, a patient with a T2* < 6 milliseconds has a 50% risk of developing heart failure in 1 year 7 (Table 2, Figure 2).

Table 2.

Grading of Myocardial Iron loading.

Grades	T2* Value (ms)
Normal	> 20
Mild to Moderate	10-20
Severe	< 10

Figure 2.

Cardiac T2 33.25 ms which is within normal limits suggesting no iron deposition.*

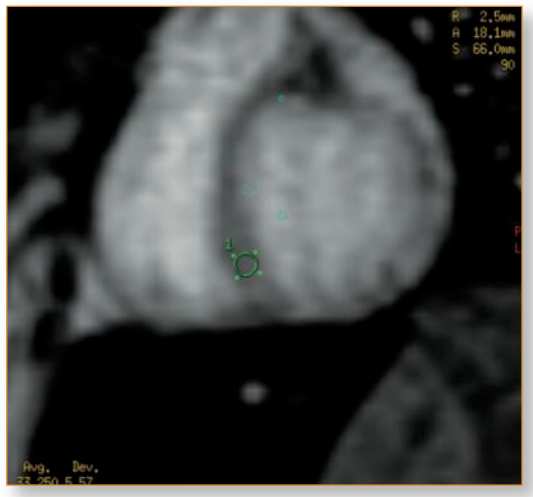

MRI assessment of pancreas

Pancreas R2* measurements can readily be obtained using the same tools and techniques used for liver R2*. Whereas they are not being used in routine clinical practice currently, pancreas R2* values offer complementary information to liver and heart iron estimates. The pancreas, like the heart, exclusively loads NTBI. The kinetics of pancreatic iron loading and unloading are intermediate between the heart and liver, making pancreas R2* a better predictor of cardiac iron than liver iron (53). Increases in pancreatic R2* can be treated as surrogates for chronic NTBI exposure and modify chelation therapy accordingly, even if cardiac and hepatic iron estimates are stable (7).
Pancreas R2* values also affect cardiac MRI monitoring strategies. Because the pancreas loads earlier than heart, a pancreas R2* value < 100 Hz essentially precludes cardiac iron deposition (negative predictive value > 95%) and these patients can be followed by abdominal MRI examination only. This staged strategy can significantly reduce MRI burden (53) (Table 3).
Both pancreas and cardiac R2* are correlated

Table 3.

Grading of pancreatic siderosis.

Grades	R2* Value (Hz)
Normal	< 30
Mild	30-100
Moderate	100-400
Severe	> 400

with glucose intolerance and diabetes. The presence of detectable cardiac iron is a relatively good predictor of overt diabetes, but lacks sensitivity for milder glucose dysregulation. Pancreas R2* > 100 Hz is sensitive for all forms of glucose dysregulation (impaired fasting glucose, impaired glucose tolerance, and diabetes), but half of these patients will have normal glucose handling. Whether pancreas R2* conveys a prospective risk of subsequent glucose dysregulation requires additional study 7.
Pancreas R2* measurements have several limitations: (1) they have not gained widespread use, (2) the staged approach to cardiac scanning has not been independently validated, (3) functional correlates require further investigation, and (4) the pancreas may be difficult to locate in older, splenectomized thalassemia major subjects because of glandular apoptosis, fatty replacement, and loss of normal anatomic landmarks (54).

MRI assessment of pitutary

With routine cardiac screening, patients are now living long enough to encounter increasing iron-mediated endocrine morbidities. Hypogonadism occurs in approximately half of thalassemia patients and has long-term consequences for fertility, bone density, and quality of life (7). Preclinical iron deposition can be detected using R2 techniques, whereas severe iron deposition is associated with decreased response to gonatropin releasing hormone challenge (55). Shrinkage of the pituitary gland is associated with more significant, irreversible loss of gonadotrophic production (56).
Further clinical validation and technical standardization is necessary before pituitary MRI can be incorporated into routine clinical monitoring, but this is an active area of research (57).

MRI assessment of adrenals

Abnormalities in adrenal function have been reported in patients with thalassaemia (58). One study evaluating adrenals for iron overload with MRI showed a significant correlation between adrenal and liver siderosis (59).
MRI assessment of spleen, lymph nodes and bone marrow
In spite of the fact that the spleen, lymph nodes and bone marrow, which all contain reticuloendothelial cells, are among the first organs to be affected by iron overload, there have been very few studies evaluating their iron overload in thalassaemia by MRI, and these used mainly SIR techniques (1). SIR of the spleen shows a significant correlation with serum ferritin but not with SIR of the liver (19). The absence of correlation between liver and spleen siderosis could be explained by differences in iron kinetics, by differences in the cluster size of iron proteins, by haemochromatosis gene mutations in β-thalassaemia major carriers, and by the presence of extramedullary haemopoietic tissue in the spleen (1).
Intraabdominal lymph nodes in β-thalassaemia have been related to chronic hepatitis C. Lymph node siderosis correlates with liver, but not with spleen siderosis (17).
In the few studies that have been reported, SIR and relaxometry methods have shown discordant results for MR parameters of bone marrow siderosis and serum ferritin (1). Normal bone marrow signal associated with liver siderosis has been reported in a few patients with thalassaemia and this may be due to differences in genotype or differences in chelation therapy regimens (16).

MRI screening protocol

Chronic packed RBC transfusion therapy increases liver iron by approximately 1 mg/mL (by dry weight) for every 15 mL/kg delivered. Therefore, patients receiving more than 10 transfusions (150 mL/kg), in the absence of significant losses, merit at least an initial scan. Cardiac iron loading is rare for patients receiving fewer than 70 units of blood, 40 so a screening abdominal examination is a reasonable initial study. Patients with high transfusion load, unknown transfusion burden, or patients with Diamond Blackfan syndrome (which exhibits early cardiac iron loading) may warrant cardiac examination on their initial visit (7).

Iron measurements should be repeated on an annual basis unless there is a clinical indication for more frequent assessment, such as the use of intensive IV deferoxamine. In patients known to be at high risk of cardiac iron, we obtain liver and cardiac studies during the same imaging session. Patients a cardiac T2* < 10 milliseconds should be evaluated at 6-month intervals given their a priori risk of cardiac decompensation (52); patients in heart failure should be scanned at 3-month intervals. Children < 7 years of age require sedation and clinicians may consider scanning every other year in this age group if trends in serum ferritin are acceptable (7).

Conclusion

Thalassemia major patients require life-long transfusion chelation to avoid premature death due to organ damage by hemosiderosis. The leading cause of death is cardiac failure, but many patients also suffer from endocrine damage such as pituitary failure, hypogonadism, diabetes mellitus, and hypothyroid and hypoparathyroidism. Even aggressive deferoxamine chelation, does not provide complete cardiac and endocrine protection. The availability of new oral iron chelating agents and T2* magnetic resonance imaging (MRI) has revolutionized thalassemia management. With the increasing options for iron chelation therapy, iron assessment by MRI can allow clinicians to more appropriately tailor chelation therapy to individual patient needs, producing greater efficacy with fewer toxicities.

References

1. *Argyropoulou MI, Astrakas L. MRI evaluation of tissue iron burden in patients with β-thalassaemia major. Pediatr Radiol 2007; 37:1191-1200.*
2. *Stark DD, Bass NM, Moss AA, et al. Nuclear magnetic resonance imaging of experimentally induced liver disease. Radiology. 1983; 148:743-751.*
3. *Wood JC. Magnetic resonance imaging measurement of iron overload. Curr Opin Hematol. 2007; 14:183-190.*
4. *Wood JC, Enriquez C, Ghugre N, et al. MRI R2 and R2* mapping accurately estimates hepatic iron concentration in transfusion-dependent thalassemia and sickle cell disease patients. Blood. 2005; 106:1460-1465.*
5. *Carpenter JP, He T, Kirk P, et al. On T2* magnetic resonance and cardiac iron. Circulation. 2011; .123:1519-1528.*
6. *St Pierre TG, Clark PR, Chua-anusorn W, et al. Noninvasive measurement and imaging of liver iron concentrations using proton magnetic resonance. Blood. 2005; 105:855-861.*
7. *John C.Wood. Impact of Iron Assessment by MRI. Hematology 2011; 443-50.*
8. *Sirlin CB, Reeder SB. Magnetic Resonance Imaging Quantification of Liver Iron. Magn Reson Imaging Clin N Am. 2010; 18:359-381.*
9. *Gandon Y, Olivie D, Guyader D, et al. Non-invasive assessment of hepatic iron stores by MRI. Lancet 2004; 363:357-362.*
10. *Kaltwasser JP, Gottschalk R, Schalk KP, et al. Non-invasive quantitation of liver iron-overload by magnetic resonance imaging. Br J Haemat. 1990; 74:360-363.*
11. *Chezmar JL, Nelson RC, Malko JA, et al. Hepatic iron overload: diagnosis and quantification by noninvasive imaging. Gastrointest Radiol. 1990; 15:27-31.*
12. *Bonkovsky HL, Slaker DP, Bills EB, et al. Usefulness and limitations of laboratory and hepatic imaging studies in iron-storage disease. Gastroenterology. 1990; 99:1079-1091.*
13. *Guyader D, Gandon Y, Robert JY, et al. Magnetic resonance imaging and assessment of liver iron content in genetic hemochromatosis. J Hepatol 1992; 15:304-308.*
14. *Gandon Y, Guyader D, Heautot JF, et al. Hemochromatosis: diagnosis and quantification of liver iron with gradient-echo MR imaging. Radiology 1994; 193:533-538.*
15. *Argyropoulou MI, Kiortsis DN, Efremidis SC .MRI of the liver and the pituitary gland in patients with beta-thalassemia major: does hepatic siderosis predict pituitary iron deposition? Eur Radiol 2003; 13:12-16.*
16. *Drakonaki EE, Maris TG, Papadakis A et al. Bone marrow changes in beta-thalassemia major: quantitative MR imaging findings and correlation with iron stores. Eur Radiol 2007; 17:2079-2087.*
17. *Papakonstantinou O, Maris TG, Kostaridou S, et al.Abdominal lymphadenopathy in beta-thalassemia: MRI features and correlation with liver iron overload and post-transfusion chronic hepatitis C. AJR 2005; 185:219-224.*
18. *Papakonstantinou O, Ladis V, Kostaridou S, et al.The pancreas in beta-thalassemia major: MR imaging features and correlation with iron stores and glucose disturbances. Eur Radiol 2006; 17:1535-1543.*
19. *Papakonstantinou O, Drakonaki EE, Maris T et al (2006) MR imaging of spleen in beta-thalassemia major. Abdom Imaging. 2006; Epub 2006 Sep 12.*
20. *Rocchi E, Cassanelli M, Borghi A, et al.Magnetic resonance imaging and different levels of iron overload in chronic liver disease. Hepatology 1993; 17:997-1002.*
21. *Gomori JM, Horev G, Tamary H et al. Hepatic iron overload: quantitative MR imaging. Radiology 1991; 179:367-369.*
22. *Gelman N, Gorell JM, Barker PB et al. MR imaging of human brain at 3.0 T: preliminary report on transverse relaxation rates and relation to estimated iron content. Radiology 1999; 210:759-767.*
23. *Ghugre NR, Enriquez CM, Coates TD et al. Improved R2* measurements in myocardial iron overload. J Magn Reson Imaging 2006; 23:9-16.*
24. *Mavrogeni SI, Markussis V, Kaklamanis L et al. A comparison of magnetic resonance imaging and cardiac biopsy in the evaluation of heart iron overload in patients with beta-thalassemia major. Eur J Haematol 2005; 75:241-247.*
25. *Aessopos A, Giakoumis A, Fragodimitri C, et al.Correlation of echocardiography parameters with cardiac magnetic reso-*

nance imaging in transfusion-dependent thalassaemia major. Eur J Haematol 2007; 78:58-65.

26. *St Pierre TG, Clark PR, Chua-Anusorn W .Measurement and mapping of liver iron concentrations using magnetic resonance imaging. Ann N Y Acad Sci 2005; 1054:379-385.*
27. *Ernst O, Sergent G, Bonvarlet P et al. Hepatic iron overload: diagnosis and quantification with MR imaging. AJR 1997; 168:1205-1208.*
28. *Alexopoulou E, Stripeli F, Baras P, et al. R2 relaxometry with MRI for the quantification of tissue iron overload in beta-thalassemic patients. J Magn Reson Imaging 2006; 23:163-170*
29. *Carr HY, Purcell EM .Effects of diffusion on free precession in nuclear magnetic resonance experiments. Phys Rev 1954; 94:630-638.*
30. *Meiboom S, Gill D.Modified spin-echo method for measuring nuclear relaxation times. Rev Sci Instrum 1958; 29:688-691*
31. *In den Kleef JJ, Cuppen JJ. RLSQ: T1, T2, and rho calculations, combining ratios and least squares. Magn Reson Med 1987; 5:513-524.*
32. *Anderson LJ, Holden S, Davis B, et al.Cardiovascular T2-star (T2*) magnetic resonance for the early diagnosis of myocardial iron overload. Eur Heart J 2001; 22:2171-2179.*
33. *Pepe A, Positano V, Santarelli MF, et al. Multislice multiecho T2* cardiovascular magnetic resonance for detection of the heterogeneous distribution of myocardial iron overload. J Magn Reson Imaging 2006; 23:662-668.*
34. *Wood JC, Tyszka JM, Carson S, et al. Myocardial iron loading in transfusion-dependent thalassemia and sickle cell disease. Blood 2004; 103:1934-1936.*
35. *Jensen PD, Jensen FT, Christensen T et al. Evaluation of myocardial iron by magnetic resonance imaging during iron chelation therapy with deferrioxamine: Indication of close relation between myocardial iron content and chelatable iron pool. Blood 2003; 101:4632-4639.*
36. *Westwood MA, Anderson LJ, Firmin DN et al. Interscanner reproducibility of cardiovascular magnetic resonance T2* measurements of tissue iron in thalassemia. J Magn Reson Imaging 2003; 18:616-620.*
37. *Gorell JM, Ordidge RJ, Brown GG, et al. Increased iron-related MRI contrast in the substantia nigra in Parkinson's disease. Neurology 1995; 45:1138-1143.*
38. *Ordidge RJ, Gorell JM, Deniau JC, et al.Assessment of relative brain iron concentrations using T2-weighted and T2*-weighted MRI at 3 Tesla. Magn Reson Med 1994; 32:335-341.*
39. *Ladis V, Chouliaras G, Berdousi H et al. Longitudinal study of survival and causes of death in patients with thalassemia major in Greece. Ann N Y Acad Sci 2005; 1054:445-450.*
40. *Kattamis A, Kassou C, Berdousi H, et al.Combined therapy with desferrioxamine and deferiprone in thalassemic patients: effect on urinary iron excretion. Haematologica 2003; 88:1423-1425.*
41. *Papakonstantinou OG, Maris TG, Kostaridou V et al. Assessment of liver iron overload by T2-quantitative magnetic resonance imaging: correlation of T2-QMRI measurements with serum ferritin concentration and histologic grading of siderosis. Magn Reson Imaging 1995; 13:967-977.*
42. *Christoforidis A, Haritandi A, Tsitouridis I, et al. Correlative study of iron accumulation in liver, myocardium, and pituitary assessed with MRI in young thalassemic patients. J Pediatr Hematol Oncol 2006; 28:311-315.*
43. *St Pierre TG, Clark PR, Chua-anusorn W, et al. Noninvasive measurement and imaging of liver iron concentrations using proton magnetic resonance. Blood 2005; 105:855-861.*
44. *Wood JC, Enriquez C, Ghugre N, et al. MRI R2 and R2* mapping accurately estimates hepatic iron concentration in transfusion-dependent thalassemia and sickle cell disease patients. Blood 2005; 106:1460-1465.*
45. *Voskaridou E, Douskou M, Terpos E et al. Magnetic resonance imaging in the evaluation of iron overload in patients with beta thalassaemia and sickle cell disease. Br J Haematol 2004; 126:736-742.*
46. *Papakonstantinou O, Kostaridou S, Maris T et al. Quantification of liver iron overload by T2 quantitative magnetic resonance imaging in thalassemia: impact of chronic hepatitis C on measurements. J Pediatr Hematol Oncol 1999; 21:142-148.*
47. *Aldouri MA, Wonke B, Hoffbrand AV et al. Iron state and hepatic disease in patients with thalassaemia major, treated with long term subcutaneous desferrioxamine. J Clin Pathol 1987; 40:1353-1359.*
48. *Kushner JP, Porter JP, Olivieri NF .Secondary iron overload. Hematology Am Soc Hematol Educ Program 2001; 47-61.*
49. *Christoforidis A, Haritandi A, Tsatra I, et al.Four-year evaluation of myocardial and liver iron assessed prospectively with serial MRI scans in young patients with beta-thalassaemia major: comparison between different chelation regimens. Eur J Haematol 2007; 78:52-57.*
50. *Cohen A .Management of iron overload in the pediatric patient. Hematol Oncol Clin North Am .1987; 1:521-544.*
51. *Porter JB, Davis BA .Monitoring chelation therapy to achieve optimal outcome in the treatment of thalassaemia. Best Pract Res Clin Haematol 2002; 15:329-368.*
52. *Kirk P, Roughton M, Porter JB, et al. Cardiac T2* magnetic resonance for prediction of cardiac complications in thalassemia major. Circulation. 2009; 120:1961-1968.*
53. *Noetzli LJ, Papudesi J, Coates TD, Wood JC. Pancreatic iron loading predicts cardiac iron loading in thalassemia major. Blood. 2009; 114:4021-4026.*
54. *de Assis RA, Ribeiro AA, Kay FU, et al. Pancreatic iron stores assessed by magnetic resonance imaging (MRI) in beta thalassemic patients. Eur J Radiol. 2012; 81: 1465-1470.*
55. *Argyropoulou MI,Metafratzi Z, Kiortsis DN, et al. T2 relaxation rate as an index of pituitary iron overload in patients with beta-thalassemia major. AJR Am J Roentgenol. 2000; 175:1567-1569.*
56. *Argyropoulou MI, Kiortsis DN, Metafratzi Z, Bitsis S, Tsatoulis A, Efremidis SC. Pituitary gland height evaluated by MR in patients with beta-thalassemia major: a marker of pituitary gland function. Neuroradiology. 2001; 43:1056-1058.*
57. *Wood JC, Noetzl L, Hyderi A, Joukar M, Coates T, Mittelman S. Predicting pituitary iron and endocrine dysfunction. AnnNY Acad Sci. 2010; 1202:123-128.*
58. *Oerter KE, Kamp GA, Munson PJ, et al.Multiple hormone deficiencies in children with hemochromatosis. J Clin Endocrinol Metab 1993; 76:357-361.*
59. *Drakonaki E, Papakonstantinou O, Maris T, et al. Adrenal glands in beta-thalassemia major: magnetic resonance (MR) imaging features and correlation with iron stores. Eur Radiol 2005; 15:2462-2468.*

Correspondence:
Kavita Saggar, MD
Dayanand Medical College - Ludhiana (India)
Email: kavita.saggar@yahoo.com